Asymmetric angular selective thermal emission

Enas Sakr*[a], Shailja Dhaka[a], Peter Bermel[a]
[a]Purdue University, School of Electrical & computer engineering, 1205 W State St., West Lafayette, Indiana, IN USA 47906

ABSTRACT

Thermal emission from blackbodies and flat metallic surfaces is non-directional, following the Lambert cosine law. However, highly directional thermal emission could be useful for improving the efficiency of a broad range of different applications, including thermophotovoltaics, spectroscopy and infra-red light sources. This is particularly true if strong symmetry breaking could ensure emission only in one particular direction. In this work, we investigate the possibility of tailoring asymmetric thermal emission using structured metasurfaces. These are built from surface grating unit elements that support asymmetric localization of thermal surface plasmon polaritons. The angular dependence of emissivity is studied using a rigorous coupled wave analysis (RCWA) of absorption, plus Kirchhoff's law of thermal radiation. It is further validated using a direct thermal simulation of emission originating from the metal. Asymmetric angular selectivity with near-blackbody emissivity is demonstrated for different shallow blazed grating structures. We study the effect of changing the period, depth and shape of the grating unit cell on the direction angle, angular spread, and magnitude of coupled radiation mode. In particular, a periodic sawtooth structure with a period of 1.5λ and angle of 8° was shown to create significant asymmetry of at least a factor of 3. Such structures can be considered arbitrary directional sources that can be carefully patterned on metallic surfaces to yield thermal lenses with designed focal lengths, targeted to particular concentration ratios. The benefit of this approach is that it can enhance the view factor between thermal emitters and receivers, without restricting the area ratio or separation distance.
Keywords: Thermophotovoltaics, directional thermal emission, plasmons, gratings

1. INTRODUCTION

The directional behavior of blackbodies is known to follow Lambert's cosine law[1], where emitted flux from a blackbody has a cosine dependence with the polar angle. Similarly, bulk thermal emitters such as metals and doped semiconductors also radiate over a wide range of angles. This in turn poses a limitation on the design of devices that depend on radiative heat transfer such as thermophotovoltaics (TPV)[2] and IR spectroscopy[3], or light sources such as LEDs[4] and incandescent light sources[5,6]. TPV devices in particular convert heat radiated by a thermal emitter into electricity using the photovoltaic (PV) effect. The efficiency of a TPV system is a function of the power spectrum of the thermal emitter, and the view factor between the emitter and the PV converter. Recent work has aimed to enhance the output TPV efficiency by matching the photonic bandgap of the emitter to the electronic bandgap of the PV diode. Prior approaches include photonic crystals and plasmonic metamaterials[7–9], as well as enhancing spectral selectivity using cold side filters[10] or integrated filters[11,12]. The angular selectivity of such structures depend on the specific design and materials. For example, a vertical 1D photonic crystal exhibits directional lobes that corresponds to the designed resonant defect mode[13], while a wide angle spectral selectivity could be maintained in a dielectric-filled 2D photonic crystal[14]. However, to maintain a high view factor, the thermal emitter should be placed in proximity to the PV diode. This arrangement requires effective cooling for the PV diode, to increase its efficiency and lifetime. Consequently, a design strategy that controls the directionality of thermal radiation is required to enhance view factors *without* restricting area ratios or separation distances between the emitter and the receiver.

*esakr@purdue.edu

Physics, Simulation, and Photonic Engineering of Photovoltaic Devices V, edited by Alexandre Freundlich, Laurent Lombez, Masakazu Sugiyama, Proc. of SPIE Vol. 9743, 97431D · © 2016 SPIE
CCC code: 0277-786X/16/$18 · doi: 10.1117/12.2211035

The goal of enhancing view factor calls for engineering thermal emitters/sources to strongly modify the direction of thermal emission. Similar design strategies were also studied for achromatic metasurface flat lenses[15] and out-of-plane focusing of surface plasmon polariton (SPP) modes[16]. Hence, the first step to achieve such an engineered emitter structure is to design highly asymmetric directional thermal sources with arbitrary directionality. There are several strategies to obtain directional thermal emission, such as 1D photonic crystals with defect modes[13], wideband Brewster angle absorption in engineered 1D photonic crystals[17] or delocalized surface modes on shallow gratings[18,19]. Also, some structures may demonstrate quasi-monochromatic, highly directional thermal emission such as plasmonic bangap structures[20], coupled resonant cavities[21], and multiple quantum well photonic crystal thermal emitters[22]. Among these techniques, highly directional far-field thermal emission from delocalized surface modes on shallow gratings is a promising approach, since a spatial angular dependence can be tailored by only changing the spatial periods over the surface, with the exception that their emission is symmetric about the normal direction. Asymmetric thermal emission utilizing evanescent coupling by double-groove Si grating placed in air above SiC has previously been reported in the mid-infrared range[23].

In this paper, we demonstrate asymmetric thermal emissivity from metallic structures in the near-infrared range, which can support nearly unidirectional SPP modes. The unit cell of metallic shallow gratings is redesigned such that it preferentially couples to only one direction of far-field radiation mode(s). This requires asymmetry in the unit cell, such that the SPP mode could be supported in one direction, thus coupled to an asymmetric radiative far-field mode. The selective angular emissivity is obtained using Kirchhoff's law of thermal radiation[1] and angular absorption simulation. We also propose a direct simulation of thermal emission with incident waves launched from the metal side, and is validated with absorption simulation. Effects of geometric parameters, including period, shape and depth is also discussed.

2. THEORY

2.1 Surface plasmon modes on metallic gratings

A delocalized SPP mode can propagate at the interface between a semi-infinite metal and air under TM excitation or p-polarization. However, the dispersion relation of the delocalized SPP mode is always below the light line, and cannot be coupled to free-space propagating modes unless a modification of the parallel momentum is introduced on the metal's surface, for example using periodic shallow gratings[5]. In this case the momentum conservation law implies a shift of the dispersion relation above the light line, and the SPP can now be probed with an incident p-polarized wave with incident angle θ_i, as given by the following relation

$$\sin\theta_i = \frac{k_\parallel}{k_0} + m\frac{\lambda}{a}, \tag{1}$$

where $k_\parallel$ is the SPP parallel wavevector at the interface, k_0 is the wavevector in air, λ is the wavelength in air and a is the grating period. This is equivalent to the conservation of crystal momentum. The order of the coupled mode is given by the integer m=±1, 2, 3, … The angular emissivity of shallow gratings can be predicted by extending Kirchhoff's law of thermal radiation with detailed balance, which implies that the angular absorptivity at a given wavelength equals the angular emissivity at the same wavelength. In other words, SPP modes on the emitter surface excited by thermal fluctuations may now be scattered by the grating elements into far-field free-space radiative modes with angle $\theta_o = \theta_i$, as described by (1). The amplitude and the full width at half maximum (FWHM) values depend on satisfying the critical coupling condition, or Q-matching condition between the absorptive and radiative loss rates[24], keeping the grating shallow enough to maintain validity of the SPP perturbation assumption. The accuracy of this assumption has been verified by comparing direct emission from the metal with absorption from air, both as a function of angle (as will be shown in Section 4).

2.2 Asymmetric unit cell

As discussed in the introduction, introducing geometric asymmetry in the unit cell has potential to support nearly unidirectional emission. To achieve this goal, we suggest a sawtooth geometry with a shallow angle. From a ray optics perspective, we can predict the behavior of the sawtooth structure upon oblique incidence excitation: an incident plane wave on the long facet of the grating will most probably experience specular reflection. On the other hand, an incident

plane wave on the vertical metallic side is much more likely to be trapped on the surface. Consequently, the probability to excite an SPP mode by incidence on the vertical surface is much greater than the probability of coupling from the grating long facet.

3. SIMULATION METHODOLOGY

To simulate the behavior of the angular emissivity for symmetric and asymmetric grating structures, we employed the rigorous coupled wave analysis (RCWA) method on a discretized structure. This method was applied to directly calculate emission and to calculate absorption. As predicted by Kirchhoff's law of thermal radiation, these two methods should be equivalent at thermal equilibrium. Further details are provided in the remainder of this section.

3.1 RCWA on a discretized sawtooth structure

We simulate angular absorption of gratings using the RCWA method combined with the s-matrix approach as implemented in the "Stanford Stratified Structure Solver" or S^4 software package developed by Liu and Fan[25]. The S^4 tool is a frequency domain solver of Maxwell's equation in multi-layer periodic structures. Since the structure involves a metallic semi-infinite substrate with surface gratings, the simulation requires a sufficient number of in-plane Fourier modes N_G to guarantee appropriate convergence of the solution[25]. The simulated unit cell of the structure is periodic with period a in the x-direction, and is infinite in the y-direction. The metallic grating layer has a depth d with a rectangular air gap of width g as shown in Fig. 1. In our case, using N_G =150 is sufficient to capture the expected SPP resonance behavior. However, there are some limitations associated with using this approach. For example, including spatial variations in the vertical direction to simulate a sawtooth structure requires discretizing the structure into a finite number of layers, each having a finite gap between their grating filling factors. This in turn can reduce the convergence speed of the structure because of the additional discontinuities associated with the discretized layers. Furthermore, the accuracy of the simulation does not necessarily increase with the number of layers, because of errors associated with the S-matrix propagation at each layer boundary. For our structures, we found that 4 layers yield the best compromise for correctly calculating the behavior of the ideal sawtooth structure. Another complexity appears from the need to use a fine step size to capture narrow angular features. However, a coarse step can be used at the beginning then a fine step can be used around the peak to obtain the correct FWHM.

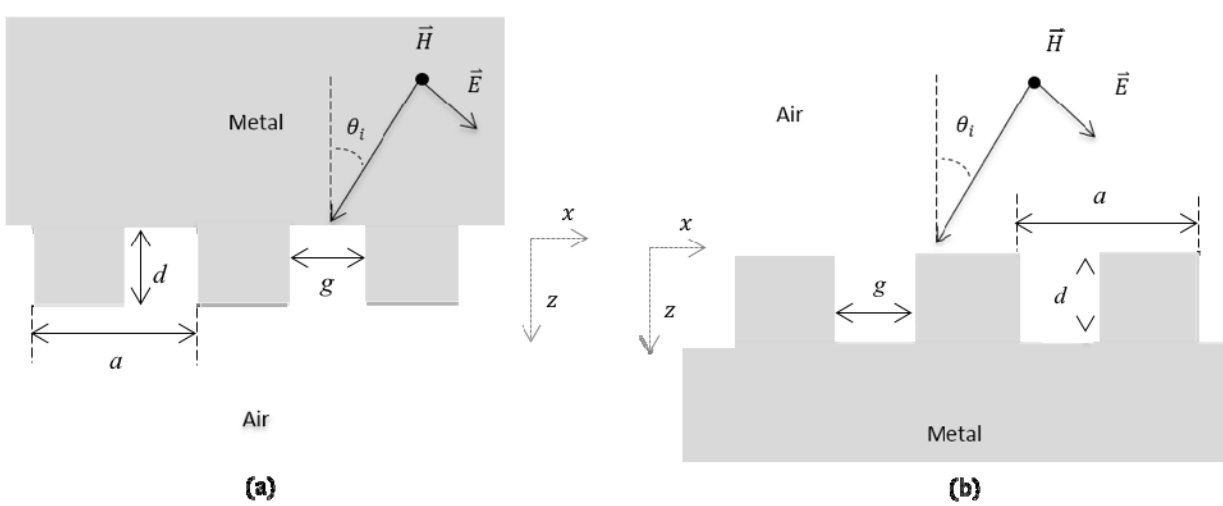

Figure 1. (a) Direct emission simulation of the lamellar grating case. Incident waves with fixed angles $\{\theta_i\}$ are launched from metal and the output waves are collected in far-field, Fourier-transformed and superimposed to compute emissivity. (b) Absorption simulation: incident waves are launched from air and $A(\theta_i) = 1 - R(\theta_i)$ is computed for each incident angle θ_i. The figure is zoomed-in in the z-direction, since $d \ll \lambda$.

3.2 Direct emission simulation

In order to simulate the direct behavior of thermal radiation process, without invoking Kirchhoff's law of thermal radiation, we excite a number of p-polarized electromagnetic modes inside the metal, just below the grating, which in

turn excite the SPP modes on the surface that get scattered by the gratings to far-field radiating modes. The procedure involves the following steps:

1. First, a number of individual simulations with incident plane waves from the metal side are created. Incident angles take values from -89° to 89° with a 1° step size.
2. The transmitted fields are measured at an *x*-*y* plane in the far-field, e.g. at a distance of 5λ, then Fourier-transformed in the spatial domain. The emission angles are characterized in the spectral domain parameter k_x with the relation $\theta_o = \mathrm{asin}(k_x/k_0)$.
3. The obtained fields are corrected for the attenuation in the *z*-direction that the incident waves suffer during propagation in the lossy metal before transmission in air. This attenuation is estimated for propagation inside the grating, using Maxwell Garnett's effective medium approximation[26]. Note that this correction is used as a first order approximation, although the size of the metallic inclusions on the surface is not very small compared to the wavelength.
4. The output power amplitudes are then computed for each incident mode, and then linearly superimposed to compute the total output power.

The simulation setup is depicted in Fig. 1(a).

3.3 Absorption simulation

A straightforward method to compute angular emissivity $\varepsilon(\theta)$ is to compute the absorptivity $A(\theta)$ at each incident angle θ_i from air, as $A(\theta) = 1 - R(\theta)$, where $R(\theta)$ is the reflectivity at θ. Kirchhoff's law with detailed balance requires that $\varepsilon(\theta) = A(\theta)$ for all matching wavelengths, angles, and polarizations. The simulation setup in this case is depicted in Fig. 1(b).

Both direct emission and absorption simulations are implemented using the Rappture toolkit[27] to be published on nanoHUB.org as the "Directional thermal emission simulation tool."[28]

4. RESULTS

4.1 Direct emission vs. absorption simulation of lamellar grating

To verify the procedure described in section 3.2, the lamellar grating case studied by Laroche et al.[19] is simulated. The metallic grating is made of Tungsten with period *a*=3 µm, air gap width *g*=1.5 µm, and depth *d*=125 µm. The optical properties of Tungsten at 4.53 µm are obtained from Rakić et al.[29] The obtained emissivity spectrum is shown on Fig. 2(a). The observed highly-directional symmetric thermal emission peaks around ±30.5° qualitatively matches the results shown in reference [19]. A maximum peak amplitude of 0.95 with FWHM of 15 mrad compares closely to experimental results of 0.8 maximum peak amplitude and 15.7 mrad[19]. The spatial Fourier transform reveals the presence of surface wave components, as well as far-field emission peaks at the corresponding angles given by (1). The procedure however shows different spurious modes for the sawtooth grating case, presumably caused by the large differences of dielectric constants across the interfaces[25]. The corresponding peak obtained by absorption simulation shows a good match to the previous results with a near unity peak amplitude and 2.3 mrad.

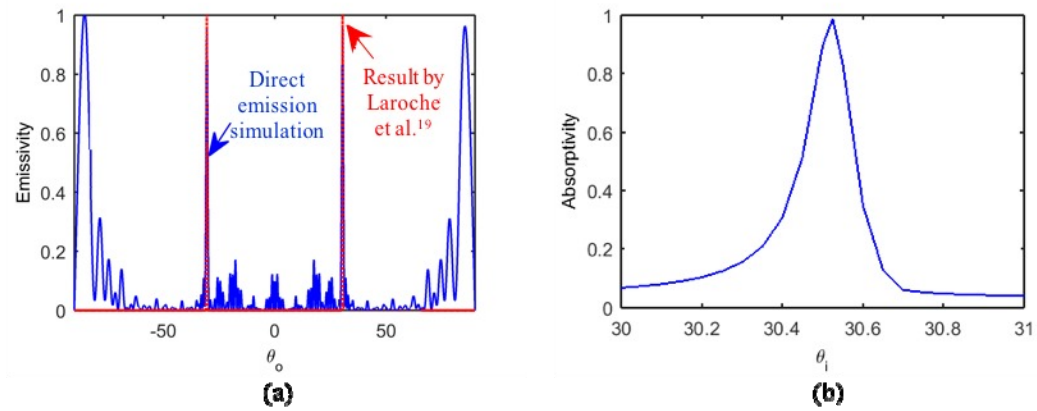

Figure 2. (a) Highly directional emission peaks obtained by direct emission simulation (blue) and qualitatively compared to previous results[19] (red). The peak emission obtained in simulation is 0.95 at 30.5°. Surface modes are noticeable near ±90°. (b) Absorption simulation result around the directional peak, in good agreement with the result obtained in (a).

4.2 Discretized sawtooth structure

Considering the sawtooth grating as a potential asymmetric emitter, the design parameters are the sawtooth angle θ_s and the period *a*. To keep a shallow grating depth *d*, small values of θ_s should be used. The typical value used in this study is 8°. The period *a* determines the direction of emission. The incident angle θ_i is defined as the angle between the direction of propagation of the incident wave and the normal direction of the corresponding planar structure as shown in the inset of Fig. 4(a). If the *x*-component of the incident wave's *k*-vector is positive, then θ_i is positive and vice versa. Initial simulation results show that the selective angular emission will remain symmetric for $\lambda/a > 1$, or when the forward and backward first order SPP modes are only supported. However, when $\lambda/a \leq 1$, higher order SPP modes can be supported, and asymmetric emission becomes evident. The simplest explanation of this phenomenon is that for $\lambda > a$, the grating will act like a periodic array of sub-wavelength scatterers, and thus the symmetry sensitivity is minimal. However, for $\lambda < a$ the symmetry sensitivity will start to take place, and the sawtooth facet will strongly reflect incident waves on it, while the vertical side will assist trapping the surface wave, and thus enhance absorption. Interestingly for the regime where $\lambda/a \leq 1$, the mode order *m* in (1) can take values larger than unity, and multiple emission peaks will appear. The most interesting regimes are at $\lambda/a = 1, 2/3, 1/2, \ldots$ etc., where the solutions of (1) intersect for two different values of *m*. In particular, at $\lambda/a = 2/3$, two definitive angular selective peaks are expected at -19.49° and 19.49°. These interesting points are labelled on Fig.3, which shows a plot of the supported emission modes by a perfect metallic periodic grating whose behavior is described by (1) when $k_{\parallel} = k_o$.

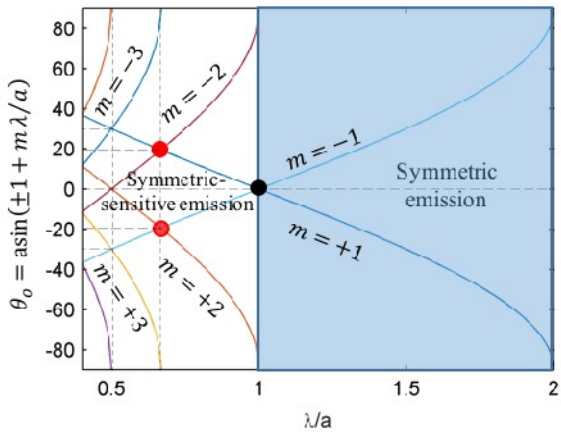

Figure 3. Expected emission modes as a function of λ/a. The emission remains symmetric for $\lambda/a > 1$ (blue region). At $\lambda/a = 1$ (black circle), emission in the normal direction is expected. For $\lambda/a < 1$, symmetric-sensitive emission takes place. At $\lambda/a = 2/3$, exactly two asymmetric modes are expected at $\pm 19.49°$ (red circles).

The asymmetric emission at $a = \lambda/0.67 \approx 1.5\lambda$ for a 4-layer discretized sawtooth grating made of Tungsten at a wavelength of 2 μm is plotted in Fig. 4(a). The dielectric constant of Tungsten here is $\epsilon = -53.4 + 20.8i$, and $\theta_s = 8°$. Two distinct peaks are observed at -19° and 19°, with amplitudes of 0.6 and 0.26, respectively, with an extinction ratio of 2.3. Furthermore, to maximize the peak amplitude, a slight modification of the geometry can be done. For example, shifting the median of the sawtooth triangular plane by 9°, while keeping the same widths of the metallic layers, as shown in the insets of Fig. 4(a), pushes the peaks values to 0.818 and 0.328, respectively, with an extinction ratio of 2.55. The peaks are centered around $\pm 21°$, since the modes begin to deviate from the intersection points (red points in Fig. 3). The scattered magnetic field profile over 4 grating periods and covering a 5 wavelength distance in air is shown in Fig. 4(b). Strong coupling of the delocalized SPP mode is evident for the -21° incidence angle (top) versus a strong scattered field in air for the 21° incidence angle case (bottom). The widths of the peaks are strongly related to the coupling between absorptive and radiative loss rates, which are functions of the metal optical properties and the dimensions of the structure.

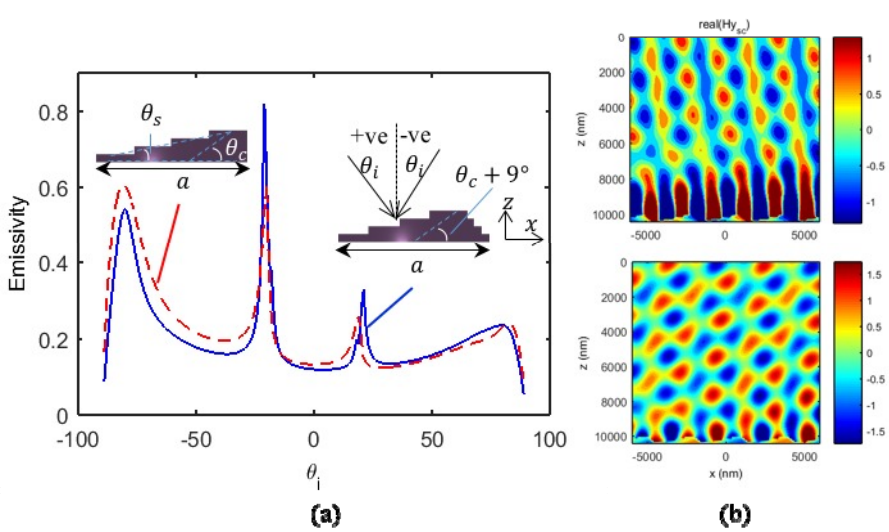

Figure 4. (a) Asymmetric emission for a Tungsten discretized sawtooth grating with $\lambda/a = 0.67$ at $\lambda = 2$ μm obtained by absorption simulation with $\theta_s = 8°$ (left inset). The -19° peak amplitude is 0.6 and the extinction ratio between peaks is 2.3. Modifying the geometry enhances the absorption through trapping the SPP mode on surface by modifying the slope of the vertical side, or alternatively, changing the median angle θ_c (right inset). The negative angle peak amplitude becomes 0.818, with extinction ratio of 2.55. (b)The scattered magnetic field profile at -21° (top) and 21° (bottom). The SPP mode is evident on the top plot, as well as the enhanced absorption.

5. CONCLUSION

We verified the directional thermal emission for a shallow lamellar grating using a direct transmission thermal emission simulation as well as absorption analysis. Both these results matched closely with prior experiments, thus validating the concept of Kirchhoff's law with detailed balance across wavelength, angle, and polarization. Based on our theoretical analysis, we also predicted asymmetric thermal emission could be achieved using asymmetric grating structures in the region where the emission wavelength is shorter than the grating periodicity. This hypothesis then led us to simulate a directional thermal emitter with asymmetric angular emission, based on delocalized surface modes on sawtooth gratings. Extinction ratio as high as 2.5 is demonstrated for directional angle of -21°. Further optimization of the geometry of the unit cell to achieve larger extinction ratios as well as near unity emissivity is still under investigation. The suggested structure is a first step to design a surface emitter with arbitrary directionality that can find applications for TPV devices and light sources. Controlling the emission spectrum is another closely connected aspect that should be jointly investigated in future work, both in terms of its basic physical behavior as well as performance optimization.

ACKNOWLEDGEMENTS

The authors would like to thank M. Ryyan Khan for providing useful code. Support was provided by the National Science Foundation Award EEC 1454315 – CAREER: Thermophotonics for Efficient Harvesting of Waste Heat as Electricity and funding from Northrop Grumman Aerospace Systems in support of "Ultra-thin metasurfaces for redirecting light and managing thermal emission." The computational resources for this work were provided by the Network of Computational Nanotechnology under NSF Award EEC-0228390.

REFERENCES

[1] Modest, M. F., [Radiative Heat Transfer], Academic Press (2013).

[2] Bauer, T., [Thermophotovoltaics: Basic Principles and Critical Aspects of System Design], Springer, Berlin (2011).

[3] Workman, J., Jr., Springsteen, A., [Applied Spectroscopy: A Compact Reference for Practitioners], Academic Press (1998).

[4] Inoue, T., Asano, T., De Zoysa, M., Oskooi, A., Noda, S., "Design of single-mode narrow-bandwidth thermal emitters for enhanced infrared light sources," J. Opt. Soc. Am. B **30**(1), 165 (2012).

[5] Ben-Abdallah, P., Marquier, F., Greffet, J.-J., "Controlling Thermal Radiation with Surface Waves," [Plasmonics: Theory and Applications], T. V. Shahbazyan and M. I. Stockman, Eds., Springer Science & Business Media, New York, 592 (2014).

[6] Ilic, O., Bermel, P., Chen, G., Joannopoulos, J. D., Celanovic, I., Soljačić, M., "Tailoring high-temperature radiation and the resurrection of the incandescent source," Nat. Nanotechnol. **advance on**, Nature Publishing Group (2016).

[7] Bermel, P., Ghebrebrhan, M., Chan, W., Yeng, Y. X., Araghchini, M., Hamam, R., Marton, C. H., Jensen, K. F., Soljačić, M., et al., "Design and global optimization of high-efficiency thermophotovoltaic systems," Opt. Express **18**, A314–A334 (2010).

[8] Rinnerbauer, V., Lenert, A., Bierman, D. M., Yeng, Y. X., Chan, W. R., Geil, R. D., Senkevich, J. J., Joannopoulos, J. D., Wang, E. N., et al., "Metallic Photonic Crystal Absorber-Emitter for Efficient Spectral Control in High-Temperature Solar Thermophotovoltaics," Adv. Energy Mater. **4**, 1400334 (2014).

[9] Liu, J., Guler, U., Li, W., Kildishev, A., Boltasseva, A., Shalaev, V. M., "High-temperature plasmonic thermal emitter for thermo-photovotaics," CLEO **1**, FM4C.5 (2014).

[10] Ortabasi, U., "Rugate Technology For Thermophotovoltaic (TPV) Applications: A New Approach To Near Perfect Filter Performance," Fifth Conf. Thermophotovoltaic Gener. Electr. **653**, 249–258, Rome, Italy (2003).

[11] Sakr, E. S., Zhou, Z., Bermel, P., "High efficiency rare-earth emitter for thermophotovoltaic applications," Appl. Phys. Lett. **105**(11), 111107 (2014).

[12] Sakr, E., Zhou, Z., Bermel, P., "Enhancing selectivity of infrared emitters through quality-factor matching," SPIE Opt. Eng. + Appl., M. Strojnik Scholl and G. Páez, Eds., 960819, International Society for Optics and Photonics (2015).

[13] Celanovic, I., Perreault, D., Kassakian, J., "Resonant-cavity enhanced thermal emission," Phys. Rev. B **72**(7), 075127 (2005).
[14] Chou, J. B., Yeng, Y. X., Lenert, A., Rinnerbauer, V., Celanovic, I., Soljačić, M., Wang, E. N., Kim, S.-G., "Design of wide-angle selective absorbers/emitters with dielectric filled metallic photonic crystals for energy applications," Opt. Express **22**(101), A144–A154 (2014).
[15] Aieta, F., Kats, M. A., Genevet, P., Capasso, F., "Multiwavelength achromatic metasurfaces by dispersive phase compensation," Science **347**(6228), 1342–1345 (2015).
[16] Kumar, M. S., Piao, X., Koo, S., Yu, S., Park, N., "Out of plane mode conversion and manipulation of Surface Plasmon Polariton Waves," Opt. Express **18**(9), 8800 (2010).
[17] Shen, Y., Ye, D., Celanovic, I., Johnson, S. G., Joannopoulos, J. D., Soljačić, M., "Optical broadband angular selectivity," Science **343**(6178), 1499–1501 (2014).
[18] Greffet, J.-J., Carminati, R., Joulain, K., Mulet, J.-P., Mainguy, S., Chen, Y., "Coherent emission of light by thermal sources.," Nature **416**(6876), 61–64, Macmillian Magazines Ltd. (2002).
[19] Laroche, M., Arnold, C., Marquier, F., Carminati, R., Greffet, J.-J., Collin, S., Bardou, N., Pelouard, J.-L., "Highly directional radiation generated by a tungsten thermal source," Opt. Lett. **30**(19), 2623 (2005).
[20] Biener, G., Dahan, N., Niv, A., Kleiner, V., Hasman, E., "Highly coherent thermal emission obtained by plasmonic bandgap structures," Appl. Phys. Lett. **92**(8), 081913 (2008).
[21] Dahan, N., Niv, A., Biener, G., Gorodetski, Y., Kleiner, V., Hasman, E., "Enhanced coherency of thermal emission: Beyond the limitation imposed by delocalized surface waves," Phys. Rev. B **76**(4), 045427 (2007).
[22] De Zoysa, M., Asano, T., Mochizuki, K., Oskooi, A., Inoue, T., Noda, S., "Conversion of broadband to narrowband thermal emission through energy recycling," Nat. Photonics **6**(8), 535–539 (2012).
[23] Ito, K., Matsui, T., Iizuka, H., "Thermal emission control by evanescent wave coupling between guided mode of resonant grating and surface phonon polariton on silicon carbide plate," Appl. Phys. Lett. **104**(5), 051127 (2014).
[24] Joannopoulos, J. D., Johnson, S. G., Winn, J. N., Meade, R. D., [Photonic Crystals Molding the Flow of Light], second, Zhurnal Eksp. i Teor. Fiz., second, Princeton University Press, Princeton, NJ (2008).
[25] Liu, V., Fan, S., "S4 : A free electromagnetic solver for layered periodic structures," Comput. Phys. Commun. **183**(10), 2233–2244 (2012).
[26] Choy, T. C., [Effective Medium Theory: Principles and Applications], Clarendon Press (1999).
[27] McLennan, M., Kennell, R., "HUBzero: A Platform for Dissemination and Collaboration in Computational Science and Engineering," Comput. Sci. Eng. **12**(2), 48–53 (2010).
[28] Dhaka, S., Sakr, E., Bermel, P., "Directional Thermal Emitter Simulation," Summer Undergrad. Res. Fellowsh. Symp., 72 (2015).
[29] Rakic, A. D., Djurišic, A. B., Elazar, J. M., Majewski, M. L., "Optical Properties of Metallic Films for Vertical-Cavity Optoelectronic Devices," Appl. Opt. **37**(22), 5271 (1998).